Temperature dependence of the second-order elastic constants of Cu-Zn-Al shape-memory alloy in its martensitic and β phases

Alfons Gonzàlez-Comas, Lluís Mañosa, and Antoni Planes
Departament d'Estructura i Constituents de la Matèria, Universitat de Barcelona, Diagonal 647, Facultat de Física, E-08028 Barcelona, Catalonia, Spain

F. C. Lovey and J. L. Pelegrina
Centro Atómico de Bariloche, 8400, San Carlos de Bariloche, Argentina

G. Guénin
Groupe d'Etudes de Métallurgie Physique et Physique des Matériaux, INSA, 20 Avenue Albert Einstein, 69621 Villeurbanne, France
(Received 30 December 1996)

The temperature dependence of the sound velocities for 13 propagation modes has been measured in a single crystal of Cu-Zn-Al monoclinic 18*R* martensite, using the pulse-echo method. By numerical procedure the complete set of nine second-order adiabatic elastic constants (C_{ij}) of the closest orthorhombic reference phase, their relative thermal variation (Γ_{ij}), and the Debye temperature (θ_D) have been obtained. The values found in the martensitic phase have been compared to data avalaible for the high-temperature bcc β-phase in the same alloy system. The velocity surfaces in the corresponding crystallographic directions of both phases have also been computed at different temperatures. It has been shown that the mechanical stability of the lattice for some particular distortions decreases as the transformation temperature is approached in both the martensitic as well as in the β phase. [S0163-1829(97)07033-1]

I. INTRODUCTION

Almost half of the elements of the periodic table and many alloys condense in the open bcc structure. With very few exceptions these bcc phases transform into a close-packed structure at lower temperature or under pressure. Although the close-packed structures are energetically more favorable, the bcc high-temperature phase is stabilized by a large vibrational entropy.[1,2] In many cases, the transition from the bcc towards the close-packed phases is displacive and first order; it is the so-called martensitic transformation.[3] Typical examples of materials undergoing martensitic transitions can be found in alkali metals, group-III and group-IV transition metals, and many noble-metal-based alloys. Among these, the Cu-based alloys have been the subject of numerous theoretical and experimental investigations due to their technologically important shape-memory properties[3] which are intimately associated with the martensitic transformation. In this paper we focus on the study of the elastic properties of the high (β) and low-temperature phases of Cu-Zn-Al, which is a typical Cu-based shape-memory alloy.

In a martensitic transformation, the lattice change can be described by shears and/or shuffles (a coordinated movement of atoms that can be expressed by a lattice wave modulation of a short wavelength, typically on the order of one to a few nearest-neighbor distances, with a characteristic wave number q).[4] Burgers[5] proposed the combination of shears in the $(110)_\beta[1\bar{1}0]_\beta$ and $(1\bar{1}2)_\beta[\bar{1}11]_\beta$ systems[6] to describe the martensitic transformation. Actually, it is expected that the lattice distortion associated with the transition occurs in such a direction where particularly a low elastic constant (and/or a phonon frequency) indicates a weak repulsive interaction for displacements. Indeed, a number of elastic anomalies preceding the martensitic transformation in the β phase have been reported, among which, the most important is a low value of the elastic modulus C' $[=(C_{11}-C_{12})/2]$, accompanied by partial softening with decreasing temperature.

Depending on composition, the low-temperature martensitic phase of Cu-Zn-Al exhibits different structures. The usual description uses the rhombohedral (R) or hexagonal (H) symmetry in the close-packed planes, and adds a number which characterizes the number of stacking sequences in the repeat unit. Following this notation, the different martensitic phases are: 3*R* and 9*R* for the rhombohedral and 2*H* for the hexagonal. Due to the absence of atomic redistributions on the lattice sites during the martensitic transformation, the martensitic phase inherits the atomic order of the high-temperature phase: this results in a doubling of the periodicity of the stacking planes for the rhombohedral phases when the β phase has the $L2_1$ configurational order. In this case the martensite is labeled 6*R* (from 3*R*) and 18*R* (from 9*R*).[7] The martensitic phase of the alloy under investigation is 18*R*. This structure is monoclinic.[8] However, for practical convenience, it is usually described as an orthorhombic lattice containing 18 close-packed atomic planes. It is worth mentioning that such a lattice is not the true Bravais lattice.[9] With respect to the orthorhombic cell, the 18*R* martensite in ternary Cu-Zn-Al alloys exhibits a further degree of monoclinicity (small),[10] which depends on alloy composition and degree of atomic order. The martensite, in this case, has the so-called ''modified 18*R* structure'' ($M18R$).[11] The Miller indices used through this work refer to this $M18R$ unit cell.

In order to gain insight on the lattice instabilities related to the martensitic transformation, it is important to experi-

mentally investigate the elastic behavior of the system on either side of the transition, i.e, the temperature dependence of the elastic constants of the β and martensitic phases. Although a number of elastic constants measurements have already been reported on single crystals of Cu-based β alloys exhibiting a martensitic transformation at low temperature,[13–15] very few measurements have been performed on the corresponding martensite. Guénin *et al.* measured the temperature dependence of the sound velocity of a limited number of modes in Cu-Zn-Al.[16] Later, Yasunaga *et al.* obtained the complete set of second-order elastic constants (SOEC) at room temperature for Cu-Al-Ni,[17] and more recently some of the present authors measured the room temperature SOEC of the 18*R* martensite in a Cu-Zn-Al alloy.[18] In this paper we report the measurement of the temperature dependence of all the elastic constants of the 18*R* martensite of a Cu-Zn-Al alloy. The paper is organized as follows: Details of the sample and experimental setup are given in Sec. II. In Sec. III A we present and discuss the temperature dependence of the SOEC on either side of the transition. In Sec. III B the velocity surfaces in the relevant crystallographic directions and their temperature dependence are represented for both phases. In Sec. III C, the SOEC are used to determine the Debye temperatures that will be used to compute the specific heat; this value is compared to data obtained using calorimetric methods. Some concluding remarks are outlined in Sec. IV.

II. EXPERIMENTAL

In the present study, a β phase single-crystal ingot of Cu-Zn-Al was grown by the Bridgman method with a nominal composition of Cu: 69.6, Zn: 12.8, and Al: 17.6 in at %.[19] The alloy of this composition transforms thermoelastically from the β-bcc phase to a monoclinic 18*R* martensite structure on cooling. Its martensitic transition temperature (M_s) has been determined to be 323 K. The single crystal was heat treated at 1073 K for 2 h, and slowly cooled in air to 343 K. In order to achieve the maximum degree of atomic order and vacancy annihilation, the sample was kept at this temperature for 3 h. After this treatment, the crystal was stressed in an Instron-type machine at 343 K, resulting in a 18*R* single crystal of martensite which was retained by cooling the specimen down to room temperature before removing the load. The lattice parameters of the *M*18*R* cell are given in Ref. 20. For the calculations we have chosen a right-handed orthogonal axial set with the y-axis parallel to the twofold b axis.

The crystal was oriented using the back-reflection Laue method and two rectangular paralellepipeds were cut for elastic-constant measurements with a low speed diamond saw: the first ($9.90\times4.15\times5.95$ mm^3) with faces perpendicular to the $[100]_M$, $[010]_M$, and $[001]_M$ directions, and the second one ($3.87\times5.05\times4.53$ mm^3) with two faces perpendicular to the $[3\bar{2}0]_M$ and $[\bar{1}\bar{2}8]_M$ directions. The samples were mechanically polished with fine grinding paper and the accuracy in the orientation of the faces was estimated to be better than 2°. Measurements of elastic constants were carried out using a pulse-echo ultrasonic method. Ultrasonic pulse transit period times were obtained using the phase-sensitive detection technique (MATEC, MBS-8000).[21] Both X-cut and Y-cut quartz transducers were used to generate and detect 5-MHz and 10-MHz ultrasonic pulses. Dow Resin 276-V9 was choosen as a bond between the specimens and the transducers for transverse and longitudinal waves. Special care was taken to ensure a correct coupling in the samples due to the small size of their faces, and a small piece of pure aluminium was used as a wave guide in some measurements. The sample was placed on a copper plate whose temperature was measured by means of an embedded Pt-100 probe of a platinum resistance thermometer. The cooling and heating runs were carried out at typical rates centered around 0.5 K min^{-1}. This rate is slow enough to ensure that the sample and the copper plate are at the same temperature. The temperature and the change in ultrasonic transit time were sequentially measured and transferred into a PC-compatible computer via GPIB. For heating and cooling rates around 0.5 K min^{-1}, a data set is taken every 0.3 K approximately. That enabled us to obtain a large amount of data for each experimental run.

III. EXPERIMENTAL RESULTS AND DISCUSSION

A. Measurement of elastic constants and their temperature dependence

Since the 18*R* martensite is monoclinic, 13 elastic constants are needed to describe its elastic behavior. However, it was found by Rodríguez *et al.*[18] that some elastic constants show values much lower than the rest of the constants, and do not play a relevant role in the description of the elastic properties of the system. It was obtained that $C_{15}, C_{25}, C_{35} \simeq 0$ within experimental error, and $C_{46} \simeq 0.3 C_{55}$, where C_{55} is the smallest of the elastic constants of the orthorhombic set. The remaining elastic constants (nine) are precisely those which are independent for a system with an orthorhombic symmetry. Therefore, the 18*R* structure can be approximated to be orthorhombic in order to simplify the description of its elastic properties. For an orthorhombic crystal the nine independent adiabatic SOEC represented in Voigt notation[22] are C_{11}, C_{12}, C_{13}, C_{22}, C_{23}, C_{33}, C_{44}, C_{55}, and C_{66}. In an anisotropic crystal the velocities of propagation of longitudinal and shear waves along different directions are related to the set of SOEC by the Christoffel equations.[23] We have measured the velocity of ultrasonic waves along 13 propagation modes; the wave vectors **k** corresponding to the directions of propagation and the components of the polarization vectors are given in Table I for all measurements. Although these measurements enable the determination of all 13 SOEC for the monoclinic symmetry, we will restrict ourselves to the orthorhombic description. The room-temperature values for the ultrasonic velocity in each mode correspond to an average over five independent runs, and the error is the maximum deviation from the mean value. The directions of propagation are expressed in terms of the Miller indices of the *M*18*R* unit cell.[24] The directions of polarization were experimentally determined: for the longitudinal modes, as the direction of propagation, and for the transverse modes from the orientation of the transducer, which was rotated until the corresponding excitation mode was obtained. This procedure resulted in considerable difficulty in obtaining some of the transverse modes; in particular, no reliable echoes were found for the modes labeled v_5

TABLE I. Experimental results for the velocity at room temperature (v_0) and its relative change with temperature $[\partial(\Delta v/v_o)/\partial T]$ for ultrasonic waves propagating with **k** and **A** as propagation vector (perpendicular to the sample surface) and polarization vector, respectively. Relationships between elastic constants and pure mode velocities are given for a number of modes.

Mode	**k**	**A**	Relationships between elastic constants and wave velocities	v_0 (ms^{-1})	$\frac{\Delta v}{\partial \frac{v}{v_o}}/\partial T$ ($10^{-3}\mathrm{K}^{-1}$)
v_1	[001]	[001]	$\rho {v_1}^2 = C_{33}$	5583±5	−0.108±0.003
v_2	[001]	[010]	$\rho {v_2}^2 = C_{44}$	2690±90	−0.064±0.005
v_3	[001]	[100]	$\rho {v_3}^2 = C_{55}$	1879±20	−0.300±0.006
v_4	[010]	[010]	$\rho {v_4}^2 = C_{22}$	4470±180	−0.178±0.006
v_5	[010]	[001]	$\rho {v_5}^2 = C_{44}$		
v_6	[010]	[100]	$\rho {v_6}^2 = C_{66}$	2228±10	−0.154±0.011
v_7	[100]	[100]	$\rho {v_7}^2 = C_{11}$	4850±60	−0.123±0.003
v_8	[100]	[010]	$\rho {v_8}^2 = C_{66}$	2521±50	0.009±0.005
v_9	[100]	[001]	$\rho {v_9}^2 = C_{55}$	1857±10	−0.307±0.004
v_{10}	$[3\bar{2}0]$	$[2\bar{1}0]$		4990±180	−0.077±0.002
v_{11}	$[3\bar{2}0]$	[231]	$v_{10}-v_{15}$ are obtained from third-order	2243±50	−0.252±0.006
v_{12}	$[3\bar{2}0]$	$[\overline{913}1]$	algebraic equations including		
v_{13}	$[\overline{1}28]$	$[\overline{913}1]$	known SOEC constants.	5000±400	−0.093±0.002
v_{14}	$[\overline{1}28]$	[801]	The resulting equations are extensive.	2800±250	−0.113±0.010
v_{15}	$[\overline{1}28]$	$[10\bar{9}1]$		1100±70	−0.483±0.016

and v_{12}. Even so, since the system of equations that gives the SOEC in terms of the velocities is overdetermined, the amount of modes measured was enough to determine the complete set of SOEC (C_{ij}). To obtain these values as best fits to the experimental determination of the ultrasonic velocities, it was necessary to use a numerical procedure based on the solution of the wave propagation equations for an orthorhombic symmetry.[23] The fact that the number of equations was larger than the number of SOEC allowed us to minimize the intrinsic error associated with the experimental nature of the coefficients. Determination of the complete set of results requires a considerable effort with the algebraic and numerical manipulation of the expressions given in Table I. We carried out this task with the help of the scientific software package MATHEMATICA™.[25] Details will not be reported here, but we have ensured the reliability of our solving methods by checking that our results are within 5% scatter coincident with those reported previously at room temperature,[18] obtained by a completely independent numerical method. The complete set of SOEC at room temperature is given in Table II.

We have measured the temperature dependence of the transit times for the modes in Table I, from about room temperature down to 220 K approximately (corrections due to thermal expansion are negligible). An example of the evolution of ultrasonic wave velocities with temperature is shown in Fig. 1. Curves are labeled according to the wave propagation and polarization directions, as indicated in Table I. The measured relative change in the velocity of the ultrasonic modes, computed by fitting a straight line to the measured

TABLE II. Averaged values of the elastic constants C_{ij} (GPa), at room temperature and at $T=M_s$, and relative thermal variation $\Gamma_{ij}={C_{ij}}^{-1}(dC_{ij}/dT)$ (10^{-4} K^{-1}), in the 18*R* martensite. Values at $T=M_s=323$ K are obtained by linear extrapolation of the experimental measured values.

$T=298$ K								
C_{11}	C_{22}	C_{33}	C_{44}	C_{55}	C_{66}	C_{12}	C_{13}	C_{23}
178 (±4)	152 (±12)	237 (±1)	55 (±4)	27 (±1)	48 (±12)	108 (±21)	41 (±32)	154 (±31)
$T=M_s=323$ K								
C_{11}	C_{22}	C_{33}	C_{44}	C_{55}	C_{66}	C_{12}	C_{13}	C_{23}
177	150	235	55	26	48	108	41	152
Γ_{11}	Γ_{22}	Γ_{33}	Γ_{44}	Γ_{55}	Γ_{66}	Γ_{12}	Γ_{13}	Γ_{23}
-2.46 (±0.06)	-3.56 (±0.13)	-2.16 (±0.07)	-1.28 (±0.11)	-6.07 (±0.10)	0.18 (±0.11)	0.88 (±0.13)	-1.88 (±0.29)	-4.3 (±0.6)

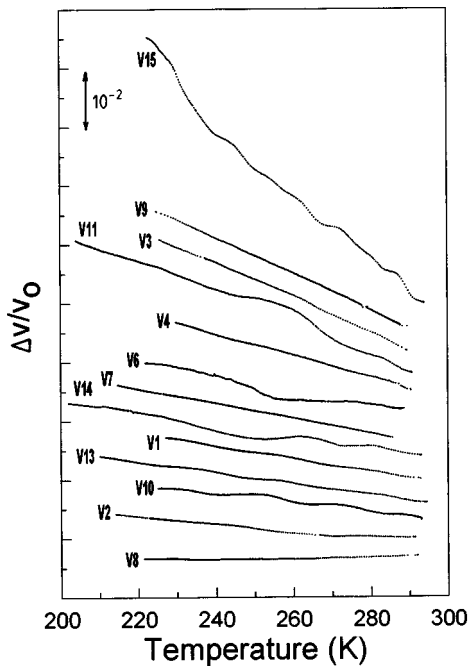

FIG. 1. Relative change in the velocity of ultrasonic waves with the temperature. v_0 is the velocity for the corresponding mode at room temperature. Curves are shifted in the vertical direction to clarify the plot, and they are labeled according to Table I.

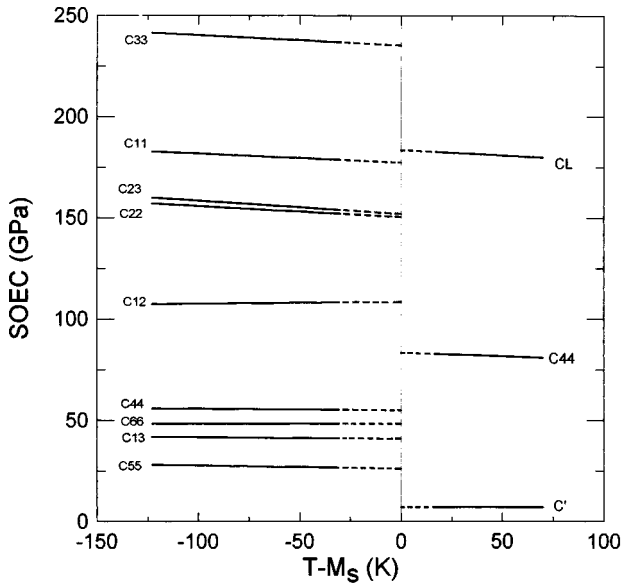

FIG. 2. Schematic comparison of the set of SOEC in the β and 18R martensite phases, given as a function of the temperature difference $T-M_s$. Data for the martensitic phase were obtained from Fig. 1 ($M_s=323$ K) and for the β phase, from Refs. 27 and 28 for $Cu_{0.677}Zn_{0.194}Al_{0.129}$ ($M_s=280$ K). Dashed lines correspond to extrapolated values in the two-phase coexistence region.

dependence, is given in Table I. It is worth pointing out that they correspond to averaged data for both cooling and heating runs. By numerically treating the data of the temperature dependence shown in Table I, we have obtained the complete set of relative thermal variation (Γ_{ij}) for all the SOEC. Results are shown in Table II.

The stability conditions for many different crystal symmetries have been developed by Cowley;[26] in the particular case of an orthorhombic crystal, C_{44}, C_{55}, C_{66}, and K_1 must be positive (K_1 is a combination of six elastic constants which cannot easily be associated with the response to a simple lattice distortion). Using the data in Table II, we have checked the behavior of the elastic constants as the sample approaches the transition: the system is stable over the whole temperature range up to M_s; relative changes between 200 K and $M_s=323$ K are: -1.55% for C_{44}, -7.04% for C_{55}, and nearly zero for C_{66}. As the sample is heated up towards the transition, the elastic constants decrease (soften), as expected from usual anharmonic theories. However, it is clear that C_{55} exhibits a larger *softening* when the temperature comes near M_s. This indicates a larger decrease in the mechanical stability of the martensitic phase for this particular shear mode. It must be stressed that C_{55} quantifies the lattice response to a shear in the $(001)_M$ plane in the $[100]_M$ direction, which is the shear system obtained from the $(110)_\beta[1\bar{1}0]_\beta$ shear in the β phase by the lattice transformation. It is instructive to compare the values of Table II with the corresponding ones in the β phase. This comparison is graphically illustrated on Fig. 2 (notice the different amount of curves making up the set of SOEC on both phases, because the change of symmetry of the alloy at the transition temperature). For the β phase, we have used the room temperature SOEC values given in Ref. 27 and the relative temperature change given in Ref. 28 The thermal hysteresis and the thermoelastic character associated with the martensitic transformation in these kinds of alloys result in a coexistence of the two phases over a temperature range. In this region, the SOEC cannot be extracted from ultrasonic data. In Fig. 2 the values in this temperature region correspond to an extrapolation (dashed lines) of the linear behavior measured in each phase. Although the composition of the alloys is slightly different from that of the sample used in the present work, this will not be relevant in the following discussion since the SOEC in β Cu-Zn-Al do not significantly depend on composition.[27] Curves in the martensitic region show negative slopes (except C_{12} and C_{66}) close to the slopes of C_L and C_{44} curves in the β-phase region. At the martensitic transition temperature, C' and C_{55} show by far the lowest value of the elastic modulus in their respective phases. There is however a remarkable difference between the values of C' and C_{55} at M_s; that is, the elastic properties exhibit a discontinuity at the transition (the jump in the velocity of the ultrasonic waves amounts to $\sim 50\%$). The results presented show that the mechanical stability of the lattice for this particular distortion exhibits the larger decrease when the sample approaches the transition from both, the martensitic and the β phases.

B. Velocity surfaces

In order to elucidate which are the relevant shears in relation to the response to all elastic distortions, it is convenient to obtain the velocity surfaces of the elastic waves. Once the complete set of elastic constants and their temperature dependence are known, the sound velocity in the corresponding crystallographic directions of the martensitic and β phases can be determined at different temperatures. These

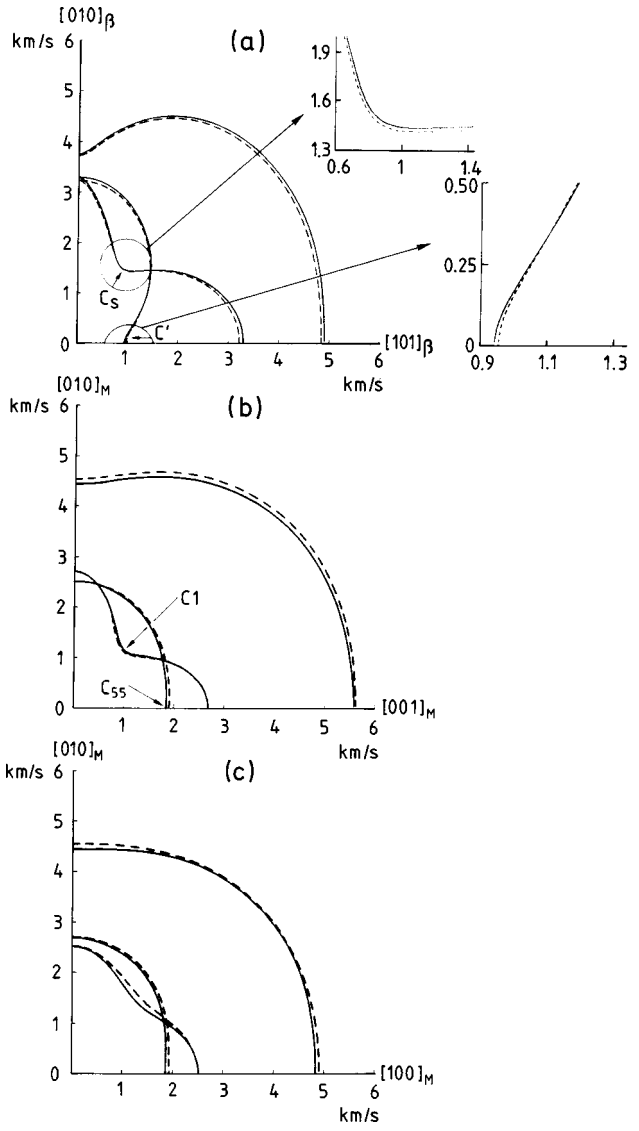

FIG. 3. Velocity surface section of the $(10\bar{1})_\beta$ plane of the β phase (a) and the corresponding $(100)_M$ (b), and $(001)_M$ (c) planes of the martensite. Solid lines correspond to $T=M_s$ and dashed lines to $T=200$ K (martensitic phase) and $T=400$ K (β phase). The outer curve in each case corresponds to the longitudinal mode, which has the highest velocity.

surfaces are obtained from the computation of the eigenvalues of the Christoffel equations for a system with orthorhombic and cubic symmetries.[22].

Figure 3(a) shows the $(10\bar{1})_\beta$ cross section of the velocity surface of the β phase, calculated from the extrapolated values of the elastic constants C_L, C_{44}, and C' at the transition temperature and at 400 K. From the figure it is apparent that velocity surfaces display a minimum value for the mode $(101)_\beta\,[10\bar{1}]_\beta$ (corresponding to the elastic constant C') and a marked dip in a direction close to the pure mode $(121)_\beta\,[1\bar{1}1]_\beta$ [associated with the elastic modulus C_s (see Ref. 29)]. As previously mentioned, these two modes are precisely the shears necessary to bring the bcc structure to the close-packed one in the Burgers picture. As temperature is reduced, all modes stiffen, with the exception of C' that softens (the mode associated with C_s shows only a very weak stiffening), see insets in Fig. 3(a). The $(101)_\beta$ plane of

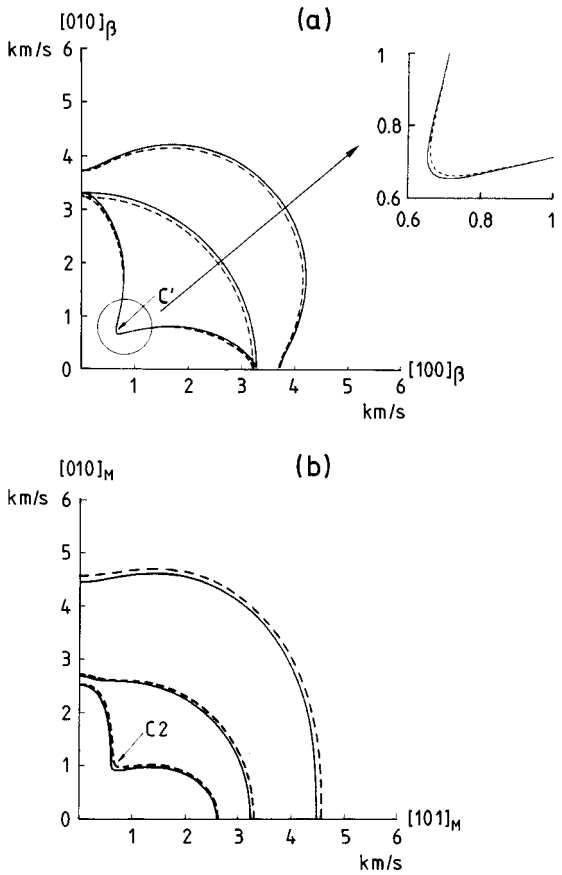

FIG. 4. Velocity surface section on the $(001)_\beta$ plane of the β phase (a) and the corresponding $(10\bar{1})_M$ (b) plane of martensite. Solid lines correspond to $T=M_s$ and dashed lines to $T=200$ K (martensitic phase) and $T=400$ K (β phase). The outer curve in each case corresponds to the longitudinal mode, which has the highest velocity.

the β phase and the equivalent $(10\bar{1})_\beta$ plane are transformed into the $(100)_M$ and $(001)_M$ planes after lattice deformation from the bcc to the orthorhombic martensite.[12] The velocity surfaces in these corresponding planes, shown in Figs. 3(b) and 3(c), exhibit qualitative features similar to those in the β phase. The velocity dip associated with C_s is still present after the transition, close to its corresponding direction of the martensite [indicated by the arrow $C1$ in Fig. 3(b)]. On the other hand, the low value of the shear mode C' in the β phase is also transferred to the martensite but with a value of the velocity significantly higher [arrow C_{55} in Fig. 3(b)]. This mode shows the larger relative decrease when the alloy approaches M_s. On the other hand, it is interesting to point out that the mode $(011)_M[01\bar{1}]_M$ (obtained by lattice transformation of the shear associated to C_s), indicated by arrow $C1$ in Fig. 3(b), stiffens on approaching the transition.

Figures 4(a) and 4(b) show the sound velocity propagating in the $(001)_\beta$ plane of the β phase and the corresponding $(10\bar{1})_M$ plane of the martensite, respectively. The dip associated with C' is indicated by an arrow in Fig. 4(a), and its temperature softening is clearly shown in the inset. The velocity surface in martensite exhibits a pronounced dip for the $(111)_M[1\bar{2}1]_M$ mode [Fig. 4(b), arrow $C2$]. This mode corresponds to a complicated combination of SOEC and comes

up from the C' shear mode $(110)_\beta[1\bar{1}0]_\beta$ in the β phase. An important feature shows up: its velocity is particularly low, lower than the velocity of the mode associated with C_{55} [see Fig. 3(b)] and it exhibits the relative larger temperature softening on approaching the transition. Actually, the symmetry change at the phase transition, breaks the degeneracy of the $\langle 110\rangle_\beta\{1\bar{1}0\}_\beta$ shears. The different shears in the martensite derived from this family exhibit low but different values for the associated elastic moduli; from all of them the $(111)_M[1\bar{2}1]_M$ mode is the one that has the lower elastic modulus at the transition temperature; in this case, the relative change in the ultrasonic velocity between the β and martensite amounts only to $\sim 17\%$ (we recall that the discontinuity with the mode associated with C_{55} is around 50%).

C. Determination of Debye temperatures

A relatively simple approach to the vibrational behavior of a solid is provided by the Debye model which considers the solid as an elastic continuum. The Debye temperature (θ_D) can be computed from the elastic properties of the solid as[30]

$$\theta_D = \left(\frac{9N}{4\pi VI}\right)^{1/3}\left(\frac{h}{k}\right), \tag{1}$$

where

$$I = \int \left(\frac{1}{{v_1}^3} + \frac{1}{{v_2}^3} + \frac{1}{{v_3}^3}\right)\frac{d\Omega}{\pi}, \tag{2}$$

and the integral is performed over the whole velocity space. Here, N is the number of atoms, V is the volume of the specimen, and the v_i (i=1,2,3) are the three velocities obtained as the eigenvalues of the wave propagation equations for a given direction. We have computed the integral I using the scientific software MATHEMATICA^{TM}. The Debye temperatures of β and martensitic phases, calculated from the room temperature elastic constants, are $\theta_D^\beta = 171$ K and $\theta_D^M = 182$ K, respectively. The estimated error in the determination of the Debye temperatures is around 10%.

We have also performed specific-heat measurements on both phases using a modulated differential scanning calorimeter, and we have compared the obtained values to those given by the Debye model using the Debye temperatures obtained from elastic constants. Calorimetric measurements render values of ${C_p}^M = 25.2$ J K^{-1} mol^{-1} and ${C_p}^\beta = 24.8$ J K^{-1} mol^{-1} for the martensitic and β phases, respectively. We estimate the error in the absolute values of heat capacities to be around 5%, but it is important to remark that the difference $\Delta C_p = 0.4$ J K^{-1} mol^{-1} between the two phases is meaningful within ± 0.1 J K^{-1} mol^{-1}. The obtained experimental values of C_p are quite comparable with those calculated from Debye theory (${C_p}^M \simeq {C_p}^\beta = 25 \pm 1$ J K^{-1} mol^{-1}). This similarity is expected to be valid at high enough temperatures. Actually, Abbé *et al.*,[31] from low-temperature C_p measurements in a β Cu-Zn-Al alloy, concluded that the Debye model was not suitable to interpret their experimental results. It is worth noticing that the application of a Debye theory with the temperatures computed from ultrasonic data does not account for the excess of entropy that is responsible for the stability of the bcc phase. The origin of this lies in the fact that a simple Debye approach does not correctly account for the low-lying TA2$[110]_\beta$ branch, which is in fact the origin of the larger vibrational entropy of bcc solids.[32]

IV. SUMMARY AND CONCLUSION

In this paper we have analyzed the elastic behavior of a Cu-Zn-Al shape memory alloy on either side of its martensitic transformation. In order to do that, we have measured the temperature dependence of the complete set of SOEC in a 18R martensite single crystal of Cu-Zn-Al. It has been found that in the martensite, all the shear modes derived from the $\langle 110\rangle_\beta\{1\bar{1}0\}_\beta$ shears of the β phase (associated with C') have particularly low values of the elastic moduli and exhibit the larger relative softening on approaching the martensitic transformation. This finding shows that the mechanical stability of the lattice for all these shears decreases when the sample approaches M_s from both sides of the transition. Among all the shear modes in the martensite, the $(111)_M[1\bar{2}1]_M$ is the one that has the lower value for the elastic modulus at the transition temperature.

ACKNOWLEDGMENTS

A.G. acknowledges financial support from DGICyT. This work has received financial support from the CICyT (Spain), Project No. MAT95-0504 and from Comissionat d'Universitats i Recerca (Catalonia), Project No. SGR119. We are also grateful to Eduard Obradó for his collaboration in the measurement of specific heats.

[1] J. Friedel, J. Phys. (France) Lett. **35**, L35 (1974).

[2] Ll. Mañosa, A. Planes, J. Ortín, and B. Martínez, Phys. Rev. B **48**, 3611 (1993).

[3] L. Delaey, in *Materials Science and Technology, Vol. 5 Phase Transformations in Materials*, edited by P. Haasen (VCH, Weinheim, 1991), p. 339.

[4] J. W. Christian, *Proceedings of the International Conference on Martensitic Transformations 1992*, edited by C.M. Wayman and J. Perkins (Monterey Institute for Advanced Studies, Monterey, 1993), p. 233.

[5] W. G. Burgers, Physica (Amsterdam) **1**, 561 (1934).

[6] We will use the subindexes β and M to denote planes and directions given in the axis of the β and martensitic phases, respectively.

[7] M. Ahlers, Prog. Mater. Sci. **30**, 135 (1986).

[8] Z. Nishiyama and S. Kajiwara, Jpn. J. Appl. Phys. **2**, 478 (1963).

[9] M. Zölliker, W. Bührer, R. Gotthardt, and J. Van Humbeeck, *The Martensitic Transformation in Science and Technology*, edited by E. Hornbogen and J. Nost (DGM, Verlag, 1989), p. 105.
[10] L. Delaey and H. Warlimont, Z. Metallkd. **56**, 437 (1965).
[11] S. Chakravorty and C. M. Wayman, Acta Metall. **25**, 989 (1977).
[12] S. Kajiwara, Mater. Trans. JIM **17**, 435 (1986).
[13] A. Nagasawa, T. Makita, and Y. Takagi, J. Phys. Soc. Jpn. **12**, 3876 (1982).
[14] Ll. Mañosa, M. Jurado, A. Planes, J. Zarestky, T. Lograsso, and C. Stassis, Phys. Rev. B **49**, 9969 (1994).
[15] A. Planes, Ll. Mañosa, D. Ríos-Jara, and J. Ortín, Phys. Rev. B **45**, 7633 (1992).
[16] G. Guénin, D. Ríos-Jara, Y. Murakami, L. Delaey, and P. F. Gobin, Scr. Metall. **13**, 289 (1979).
[17] M. Yasunaga, Y. Funatsu, S. Kojima, K. Otsuka, and T. Suzuki, Scr. Metall. **17**, 1091 (1983).
[18] P. L. Rodríguez, F. C. Lovey, G. Guénin, J. L. Pelegrina, M. Sade, and M. Morin, Acta Metall. Mater. **41**, 3307 (1993).
[19] The samples investigated are the same as those used in Ref. 18.
[20] G. Guénin, R. Pynn, D. Ríos-Jara, L. Delaey, and P. F. Gobin, Phys. Status Solidi A **59**, 553 (1980).
[21] R. C. Williamson, J. Acoust. Soc. Am. **45**, 1251 (1982).
[22] J. F. Nye, *Physical Properties of Crystals* (Oxford University Press, Oxford, 1987), p. 140.
[23] V. A. Shutilov, *Fundamental Physics of Ultrasound* (Gordon and Breach, Amsterdam, 1988), p. 304.
[24] F. C. Lovey, Acta Metall. **35**, 1103 (1987).
[25] S. Wolfram, *Mathematica* (Addison-Wesley, Reading, MA 1991).
[26] R. A. Cowley, Phys. Rev. B **13**, 4877 (1976).
[27] T. Suzuki, Y. Fujii, R. Kojima, and A. Nagasawa, *Proceedings of the International Conference on Martensitic Transformations 1986*, Nara (The Japan Institute of Metals, Sendai, 1986), p. 874.
[28] G. Guénin, M. Morin, P. F. Gobin, W. Dejonghe, and L. Delaey, Scr. Metall. **11**, 1071 (1977).
[29] A. Planes, Ll. Mañosa, and E. Vives, Phys. Rev. B **53**, 3039 (1996).
[30] H. B. Huntington, *Solid State Physics: Advances in Research and Applications* (Academic, New York, 1958), Vol. 7, p. 253.
[31] D. Abbé, R. Caudron, and R. Pynn, J. Phys. F **14** , 1117 (1984).
[32] W. Petry, J. Phys. (France) IV **5**, C2-15 (1995).